Biochemical and Biophysical Research Communications **268,** 82–87 (2000)
doi:10.1006/bbrc.1999.2058, available online at http://www.idealibrary.com on IDEAL®

Concentration of Caveolin-1 in the Cleavage Furrow as Revealed by Time-Lapse Analysis

Hiroshi Kogo[1] and Toyoshi Fujimoto

Department of Anatomy and Molecular Cell Biology, Nagoya University School of Medicine, Showa-ku, Nagoya 466-8550, Japan

Received December 21, 1999

Caveolin-1 is a major component of caveolae. Recent studies have suggested a possible role of caveolin-1 in cell transformation and normal cell proliferation. To observe the behavior of caveolin-1 in living mitotic cells, we prepared cDNA constructs encoding the chimeric protein of α- or β-caveolin-1 and green fluorescent protein (GFP) and transfected culture cells with them. Correct targeting of the chimera to the caveolae was confirmed by colocalization with the caveolar inositol 1,4,5-trisphosphate receptor-like protein. By time-lapse observation of mitotic MDCKII cells, the GFP–caveolin-1 chimeras were seen throughout the plasma membrane before cell division, but became markedly concentrated at the cleavage furrow during cytokinesis. Accumulation around the spindle poles was also observed at late telophase. The result showed that caveolin-1 undergoes a drastic distributional change during cell division and suggested that the protein may be involved in the cytokinetic process.

Caveolae are small invaginations of the plasma membrane, and have been proposed to have roles in transcytosis of macromolecules in endothelial cells (1). Recent studies on the protein composition of caveolae and/or caveolar-like membranes revealed the existence of many molecules including lipid-modified signaling molecules (Src-like kinases, H-ras, endothelial nitric-oxide synthase, and G-proteins), receptor tyrosine kinases (epidermal growth factor receptor, platelet-derived growth factor receptor, and insulin receptor), inositol 1,4,5-trisphosphate (IP3) receptor-like protein, and plasmalemmal Ca^{2+} pump, and several hypotheses have been proposed for the caveolar function (2–4).

Caveolin-1 was identified as a major component of caveolae (5), and two isoforms of caveolin-1 (α and β) were shown to be produced by alternative translation initiation (6). Recent studies on the properties of caveolin-1 demonstrated many possible functions of this molecule including cholesterol transport (7, 8), inhibitory interaction with signaling molecules (9), and suppression of oncogenic transformation (10). In the caveolin-1 molecule, the cytoplasmic membrane-proximal region was demonstrated to be critical for oligomerization and the interaction with a variety of proteins, and termed as the caveolin scaffolding domain (11). By the identification of a motif sequence that binds to the caveolin scaffolding domain, possible interaction between caveolin-1 and other proteins was suggested (12). These findings suggest multiple roles of caveolin-1 in many cell functions.

Notably, recent studies demonstrated the involvement of caveolae and caveolin-1 in cell growth and transformation. Caveolin-1 was first identified as a major v-Src substrate in Rous sarcoma virus-transformed cells (13). The finding that the caveolin-1 expression and caveola formation were markedly reduced in NIH 3T3 cells transformed by v-Abl or H-ras (G12V) suggested a critical role of caveolae in oncogenic transformation (14). Consistent with this, the recombinant expression of caveolin-1 resulted in *de novo* formation of caveolae, and abrogated the anchorage-independent growth of the transformed NIH 3T3 cells (10). Moreover, the reduction of the caveolin-1 expression by an antisense method led to cell transformation and hyperactivation of the mitogen-activated protein (MAP) kinase cascade (15); caveolar localization of MAP kinase cascade molecules (16) and inhibition of their kinase activity by caveolin-1 (17) were also demonstrated.

Lee *et al.* (18) reported that the expression of α-caveolin-1 changed during the cell cycle and was maximal during the G2/M phase in normal human mammary epithelial cells. This result suggests that caveolin-1 also plays some role in normal cell proliferation. If caveolae and caveolin-1 are functionally related to cell-cycle progression, they may show a different localization at different phases. To keep track of

[1] To whom correspondence should be addressed. Fax: (81)-52-744-2011. E-mail: hkogo@med.nagoya-u.ac.jp.

0006-291X/00 $35.00

possible distributional changes, we constructed green fluorescent protein (GFP)-caveolin-1 chimeras and observed their dynamic behavior in dividing cells. Notably, a marked concentration was observed at the cleavage furrow during cytokinesis. Recently, after our work had been completed, another group reported a study using GFP-caveolin-1 chimera, and they dealt with the relationship with cell-cell contact (19). The implication of our observations are discussed herein in relation to caveolin-1 functions in cell proliferation.

MATERIALS AND METHODS

Plasmid construction of GFP-caveolin-1 chimera. The cDNA encoding full-length human α- and β-caveolin-1 was obtained by PCR using a human umbilical vein endothelial cell cDNA library as a template with the combination of the following primers: 5′-end sense for α-caveolin-1 (5′-AAGCTTAGCATGTCTGGGGGCAAATAC-3′), 5′-end sense for β-caveolin-1 (5′-AAGCTTCAAGGCCATGGCAGACGAG-3′), 3′-end antisense without stop codon (5′-CTGCAGTATTTCTTTCTGCAAGTTGATGC-3′), and 3′-end antisense with stop codon (5′-GAATTCATATTTCTTTCTGCAAGTTGATG-3′). The PCR products without a stop codon were subcloned into pEGFP-N1 (CLONTECH) for the expression of chimeric protein, α- or β-caveolin-1/GFP; and GFP was fused to the C terminus of α- or β-caveolin-1. Whereas those with a stop codon were subcloned into pEGFP-C3 (CLONTECH) for the expression of GFP/α- or β-caveolin-1; and GFP was fused to the N terminus of α- or β-caveolin-1.

Cell culture and transfection. MDCKII and Pam212 (20) cells were kindly provided by Dr. Kai Simons (EMBL, Germany) and Dr. Koji Hashimoto (Ehime Univ., Japan), respectively. COS7 cells were obtained from the Japanese Cancer Resources Research Bank (Tokyo, Japan). Cells were grown at 37°C in 5% CO_2 in Dulbecco's modified Eagles minimum essential medium (Nihonseiyaku Co.) supplemented with 10% fetal bovine serum, 50 U/ml penicillin, and 0.05 mg/ml streptomycin. Transfection by the plasmid construct was performed with a lipofection reagent, DOTAP (Boehringer-Mannheim) or SuperFect (QIAGEN), with 2 μg of DNA/35-mm dish as instructed by the manufacturer's manual. Stably transfected MDCKII cells were selected with G418 (500 μg/ml) and cloned.

Antibodies. Rat monoclonal antibody to cerebellar P400 protein (4C11) was kindly provided by Dr. Katsuhiko Mikoshiba (Univ. of Tokyo) (21). Rabbit anti-caveolin-1 polyclonal antibody (C13630, Transduction Laboratories), mouse anti-caveolin-1 monoclonal antibody (2234, Transduction Laboratories), and rabbit anti-GFP polyclonal antibody (CLONTECH) were obtained commercially.

Immunofluorescence microscopy. COS7 and Pam212 cells cultured on glass coverslips were transiently transfected with pEGFP-N1 or α-caveolin-1-pEGFP-N1, and fixed with 3% formaldehyde in 0.1 M sodium phosphate buffer, pH 7.4, for 5–10 min at room temperature (r.t.). The cells were permeabilized with 0.1% Triton X-100 in PBS for 5 min, treated with 3% BSA in PBS for 10 min, and incubated with mAb 4C11 for 1 h and then with rhodamine-conjugated goat anti-rat IgG antibody for 30 min, all at r.t. The specimens were mounted with a glycerol/Mowiol 4-88 (Calbiochem–Novabiochem Corp.) mixture containing 1,4-diazobicyclo-[2,2,2]-octane (Eastman Kodak Co.) and observed under a Zeiss Axioplan fluorescence microscope (Carl Zeiss, Inc.).

Western blotting. Cells were rinsed with ice-cold PBS twice, and treated with 10% trichloroacetic acid on ice for 10 min before being boiled in an SDS sample buffer (150 mM Tris–HCl, 20% sucrose, 2.5% SDS, and 2% 2-mercaptoethanol; pH 6.8). The proteins were separated by SDS–PAGE (5–15% gradient acrylamide gel) and transferred onto a nitrocellulose membrane (Hybond ECL, Amersham). The blotted membranes were blocked with 5% skim milk, 0.1% Tween 20 in PBS overnight, and then incubated with anti-caveolin-1 or anti-GFP antibody for 3 h at r.t. and subsequently with goat anti-rabbit antibody conjugated with horseradish peroxidase. The signal was detected with the ECL detection system (Amersham) according to the instruction manual.

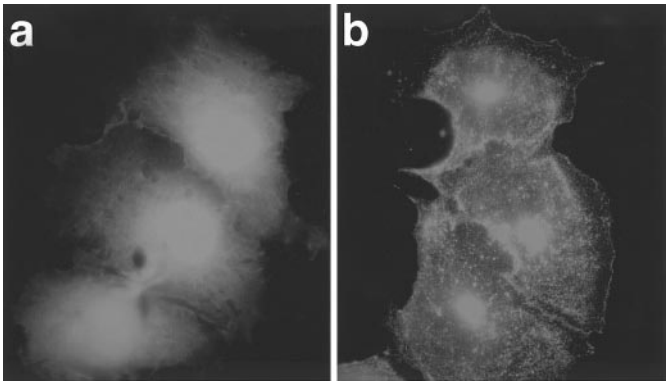

FIG. 1. Distribution of GFP (a) and α-caveolin-1/GFP (b) expressed in COS7 cells. GFP alone showed a diffuse distribution throughout the entire cytoplasm and nucleus, whereas the caveolin-1 chimera was observed as distinct dots in the cytoplasm. Bar, 10 μm.

Time-lapse analysis. The MDCKII cells stably transfected with the GFP constructs were cultured in glass-bottomed dishes and observed with a Zeiss Axiovert 135 fluorescence microscope (Carl Zeiss, Inc.). The medium was buffered with 25 mM Hepes, and the temperature was kept at 37°C with an electric thermostat system (DTC-200, DIA Medical System, Co.) during observation. Images were captured every 60 seconds for 60 min by a chilled CCD camera connected to an Argus-20 image processor and a time-lapse data collection system (Hamamatsu Photonics).

Enrichment for mitotic cells. The MDCKII cells stably transfected with α-caveolin-1-pEGFP-N1 were treated with 0.5 mM hydroxyurea for 14 h to block the cell cycle at early S phase (22). The cells were washed and kept in culture for 8 h before fixation with 3% formaldehyde in 0.1 M sodium phosphate buffer, pH 7.4. The nuclei of the cells were stained with 4′,6-diamidino-2-phenylindole (DAPI) and observed under a fluorescence microscope to identify the mitotic stage of the cells.

RESULTS

We prepared four different cDNA constructs for the present experiment: GFP was attached to either the N or C terminus of the two isoforms (α and β) of caveolin-1. The relative position of GFP was changed because masking of a particular position of the caveolin-1 molecule might cause artificial results, and the two isoforms were compared to study possible differences between them. As a result, however, all four constructs showed virtually the same localization and behavior, and thus in the following section, we will describe the results for α-caveolin-1/GFP, that is, the chimera with GFP attached to the C terminus of α-caveolin-1.

In COS7 cells, α-caveolin-1/GFP was observed as distinct dots in the cytoplasm (Fig. 1b), whereas GFP alone existed in a diffuse state throughout the cyto-

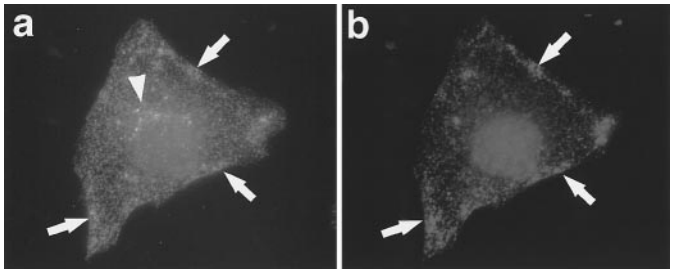

FIG. 2. Distribution of α-caveolin-1/GFP (a) and the caveolar IP3 receptor-like protein (b) in Pam212 cells transiently transfected with α-caveolin-1-pEGFP-N1. The two proteins showed colocalization (arrows) except for the perinuclear distribution of α-caveolin-1/GFP (a, arrowhead). Bar, 10 μm.

plasm and in the nuclei (Fig. 1a). To confirm the correct targeting of α-caveolin-1/GFP to caveolae, we stained Pam212 cells transiently expressing α-caveolin-1/GFP with 4C11, a monoclonal antibody that recognizes the caveolar IP3 receptor-like protein (23). The distribution of α-caveolin-1/GFP (Fig. 2a) and the immunofluorescence of 4C11 (Fig. 2b) matched each other except that α-caveolin-1/GFP was localized in the perinuclear region additionally (Fig. 2a, arrowhead).

MDCKII cells stably transfected with each chimeric construct of caveolin-1 and GFP were established by G418 selection, and expression of the recombinant proteins was confirmed by Western blotting with anti-caveolin-1 and anti-GFP antibodies. In the cells transfected with α-caveolin-1-pEGFP-N1, 52- and 48-kDa bands were recognized with both antibodies (Fig. 3, arrowheads in lane 2), probably corresponding to α- and β-caveolin-1/GFP produced by alternative translation initiation. The lower band was at the same position as that detected in the cells transfected with β-caveolin-1-pEGFP-N1 (Fig. 3, lane 3). In the cells transfected with α- or β-caveolin-1-pEGFP-C3, only a single band was detected at the expected sizes (Fig. 3, arrowheads in lanes 4 and 5). The size of the expressed chimera proteins was slightly different depending on the location of the GFP tag (whether tagged at the N or C terminus); the difference can be explained by the length of linkage between GFP and caveolin-1. With anti-caveolin-1 antibody, endogenous caveolin-1 was detected intensely in all of the clones (Fig. 3, arrow).

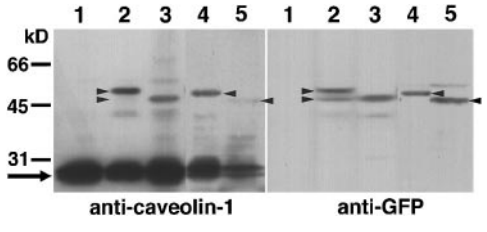

FIG. 3. Western blot analysis of MDCKII cells stably transfected with the plasmid encoding GFP-caveolin-1 chimeras. Lane 1, no transfection; lane 2, α-caveolin-1-pEGFP-N1; lane 3, β-caveolin-1-pEGFP-N1; lane 4, α-caveolin-1-pEGFP-C3; lane 5, β-caveolin-1-pEGFP-C3. 52- and 48-kDa bands were detected (arrowheads in lane 2) in the cells transfected with α-caveolin-1-pEGFP-N1. The size of the lower band was identical to the band expressed in the cells transfected with β-caveolin-1-pEGFP-N1 (lane 3). Only a single band was detected in the cells transfected with α- or β-caveolin-1-pEGFP-C3, at 51 or 47 kDa, respectively (arrowheads in lanes 4 and 5). Endogenous caveolin-1 was intensely labeled in all of the clones (arrow).

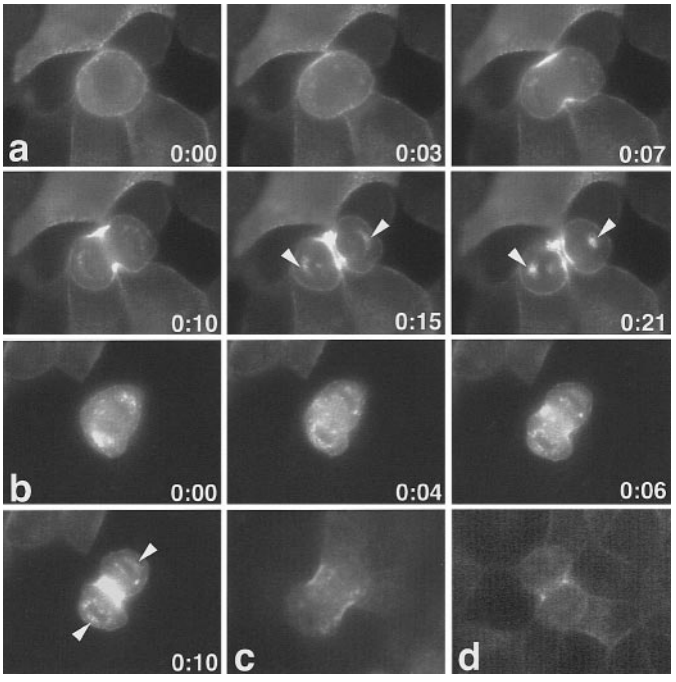

FIG. 4. The time-lapse observation of GFP-caveolin-1 chimeras in living mitotic MDCKII cells. (a) Photographs of MDCKII cells transfected with α-caveolin-1-pEGFP-N1 and photographed at 0, 3, 7, 10, 15, and 21 min after the start of recording. Before cytokinesis, α-caveolin-1/GFP was observed throughout the plasma membrane (0:00). During cytokinesis, α-caveolin-1/GFP was gradually recruited to the cleavage furrow (0:03–0:15). Another accumulation was also observed around the spindle poles toward the end of cytokinesis (arrowheads at 0:15 and 0:21). (b) Photographs of MDCKII cells transfected with β-caveolin-1-pEGFP-N1; the photos were taken at 0, 4, 6, and 10 min after the start of recording. The accumulation in the cleavage furrow was also observed for β-caveolin-1/GFP. c and d. Photographs of MDCKII cells in cytokinesis transfected with α-caveolin-1-pEGFP-C3 (c) and β-caveolin-1-pEGFP-C3 (d). The concentration in the cleavage furrow was also observed with the chimeras in which GFP had been fused to the N terminus of caveolin-1.

The behavior of α-caveolin-1/GFP in living mitotic MDCKII cells was observed by time-lapse recording. In rounded cells before cytokinesis, α-caveolin-1/GFP with GFP attached to the C terminus was localized all around the cell surface (Fig. 4a, 0:00). At the beginning of cytokinesis (Fig. 4a, 0:03), a slight concentration of the GFP signal was observed at the forming furrow; and as the division progressed, α-caveolin-1/GFP was prominently concentrated in the cleavage furrow (Fig. 4a, 0:07–0:15). The accumulation became apparent just at the beginning of the furrow formation or shortly

after it. In the late phase of cytokinesis, another prominent concentration of the signal was observed near the spindle poles (Fig. 4a, arrowheads). The β-caveolin-1/GFP also showed a similar concentration in the cleavage furrow (Fig. 4b, 0:00–010) and at the spindle pole (Fig. 4b, 0:10, arrowheads), indicating that there is no behavioral difference between the two isoforms during cytokinesis. The accumulation of GFP signals at the furrow was also observed with GFP/α-caveolin-1 and GFP/β-caveolin-1 in which the fluorescent tag had been fused to the N terminus (Figs. 4c and 4d, respectively).

The localization of α-caveolin-1/GFP during mitosis was also observed (Fig. 5, left column) in fixed MDCKII cells with reference to the mitotic stages of the nucleus stained with DAPI (Fig. 5, right column). In prophase (Fig. 5a) and metaphase (Fig. 5b), α-caveolin-1/GFP was localized throughout the plasma membrane and sometimes around centrioles (Figs. 5a and 5b, arrowhead). In early anaphase (Fig. 5c), the concentration of the GFP chimera was not yet observed at the equator. The concentration of the chimera at the furrow was observed in all of the cells during cytokinesis ($n = 9$) (Figs. 5d and 5e). The perinuclear concentration was evident toward the end of cytokinesis (Figs. 5e and 5f, arrowheads).

DISCUSSION

To exclude the possibility that the chimeric proteins may have resulted in the incorrect targeting by masking a particular end of caveolin-1 with GFP, we prepared cDNA constructs having GFP fused to either terminus of the caveolin-1 molecule. As a result, all the constructs showed the same localization and behavior in the present experiment, indicating that the possibility of artificial targeting was minimal.

We tried to detect the endogenous caveolin-1 in mitotic cells by an immunofluorescence method with anti-caveolin-1 antibodies, C13630 and 2234, one recognizing both α and β isoforms, and other the α-isoform alone. However, the strong concentration in the cleavage furrow comparable to that of the GFP chimera was not detected; only weak concentration of the signal was detected in about 40% of the cytokinetic cells examined. The reason for this difficulty in detecting endogenous caveolin-1 in the furrow is not known. A lower signal-to-noise ratio of the indirect immunofluorescence staining than the GFP signal may be a possibility. Another possible explanation is that caveolin-1 in the furrow may not be efficiently recognized by the antibodies for some unknown reason, for it was reported that recognition by antibodies was affected by the subcellular localization of caveolin-1 (24).

The prominent concentration of caveolin-1 in the cleavage furrow of MDCKII cells strongly suggests a possible function of caveolin-1 in the cytokinetic process. Caveolin-1 is known to interact directly with various molecules and modulate their functions through the caveolin scaffolding domain (9). Thus caveolin-1 might function as a regulator of the cytokinesis-associated signaling molecules. In particular, caveolin-1 is thought to be a general kinase inhibitor, interacting

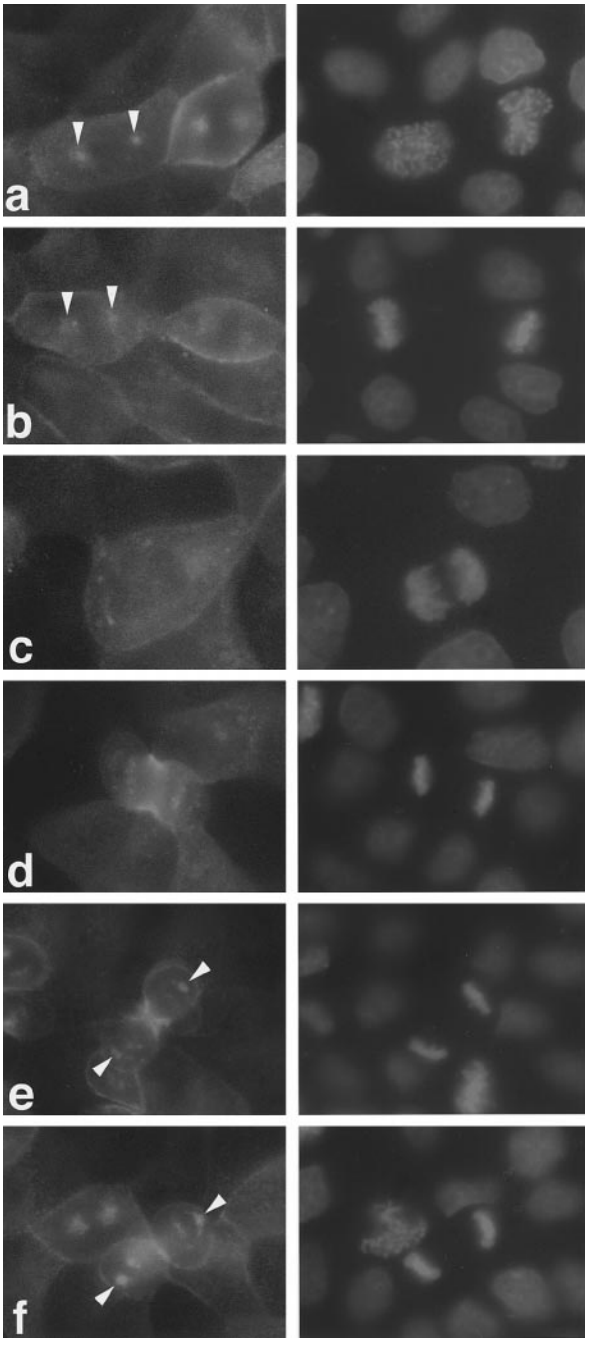

FIG. 5. Comparative observation of α-caveolin-1/GFP (left column) and chromosomes (right column) in mitotic MDCKII cells. (a) Prophase, (b) metaphase, (c) anaphase, (d–f) telophase. At prophase and metaphase, α-caveolin-1/GFP was distributed throughout the plasma membrane and around centrioles (arrowheads in a and b). As cytokinesis occurred, the chimera accumulated at the cleavage furrow (d–f); concentration around the spindle poles was observed at late telophase (arrowheads in e and f).

with the consensus sequence termed "caveolin-binding motif," present in the catalytic domain of many tyrosine and serine/threonine protein kinases (9). In cytokinesis, protein kinases are thought to play important roles (24, 25). For example, the small GTPase rho, which controls the organization of actin-related structures (26), and its target proteins, such as Rho-kinase and citron kinase, were reported to be essential in cytokinesis (27–29); and the caveolin-binding motif was found in the kinase domain of the Rho-kinase, although the interaction was not proved. A recent study also demonstrated the concentration of RhoA in caveolae (30). Besides signaling molecules, myosin II was copurified with caveolins in the caveolin-rich membrane fraction (31); and the direct interaction of caveolin-1 and myosin II was suggested based on the presence of some caveolin-binding motifs in the latter (12). These results imply that caveolin-1 may function as a regulatory protein of the phosphorylation signaling and actomyosin contraction in the cleavage furrow. In the present study, it was not determined whether caveolae as a whole are concentrated in the cleavage furrow. In fact, marked concentration of caveolae invaginations was not observed in the cleavage furrow by electron microscopy (data not shown). However, as caveolae are known to lose their invagination in some conditions (32), a possibility that shallow or flat caveolae may exist in the furrow could not be excluded; further studies using other caveolae markers are necessary to answer this question.

The intracellular location of GFP-caveolin-1 chimeras near the spindle pole at the late stage of cell division was not determined, but apparently one possibility is the Golgi apparatus, which becomes fragmented during mitosis and recovers to its original configuration at telophase. An alternative possibility is the accumulation of internalized caveolae membranes, which was reported to occur around the spindle pole of mitotic MDCK cells (33); a similar membrane was observed in cells treated with okadaic acid (33), which induces the mitotic state (34). If the latter possibility is the case, the physiological function of the caveolae internalization at the end of mitosis would be an interesting question to be studied.

The concentration of the GFP-caveolin-1 chimeras in the cleavage furrow was not a general phenomenon among the examined cells. A similar, but less prominent, concentration was seen in CHO cells, but not obvious in Pam212 cells (data not shown). In PtK2 cells, the GFP-caveolin-1 chimera was transiently concentrated at the equatorial plane just after the chromosomal segregation and disappeared before cytokinesis (data not shown). The reason for this discrepancy among cell types is not apparent; the contribution of caveolin-1 in the cytokinetic event may be divergent in different cell types. The polarized distribution of caveolins in MDCKII cells (35) may be related to the prominent concentration of caveolin-1 in the cleavage furrow. Supporting this interpretation, the concentration of GFP-caveolin-1 chimeras in the furrow was conspicuous in MDCKII cells cultured at confluence in which state the polarity is established, but not so in the cells cultured sparsely (data not shown).

To conclude, using GFP chimeras we demonstrated the prominent recruitment of caveolin-1 in the cleavage furrow of mitotic MDCKII cells. No direct evidence showing the role of caveolae and caveolin-1 in cytokinesis was obtained, but the results imply their possible function in the process. Caveolin-1 may be related to cell-cycle progression, not only by interacting with the MAP kinase cascade as previously reported (15), but also by regulating the cytokinetic process.

REFERENCES

1. Parade, G. E. (1960) *Anat. Rec.* **136,** 254.
2. Lisanti, M. P., Sherer, P. E., Tang, Z.-L., and Sargiacomo, M. (1994) *Trends Cell Biol.* **4,** 231–235.
3. Shaul, P. W., and Anderson, R. G. W. (1998) *Am. J. Physiol.* **275,** L843–L851.
4. Fujimoto, T., Hagiwara, H., Aoki, T., Kogo, H., and Nomura, R. (1998) *J. Electron Microsc. Tokyo* **47,** 451–460.
5. Rothberg, K. G., Heuser, J. E., Donzell, W. C., Ying, Y. S., Glenney, J. R., and Anderson, R. G. W. (1992) *Cell* **68,** 673–682.
6. Scherer, P. E., Tang, Z., Chun, M., Sargiacomo, M., Lodish, H. F., and Lisanti, M. P. (1995) *J. Biol. Chem.* **270,** 16395–16401.
7. Murata, M., Peranen, J., Schreiner, R., Wieland, F., Kurzchalia, T. V., and Simons, K. (1995) *Proc. Natl. Acad. Sci. USA* **92,** 10339–10343.
8. Smart, E. J., Ying, Y., Donzell, W. C., and Anderson, R. G. W. (1996) *J. Biol. Chem.* **271,** 29427–29435.
9. Okamoto, T., Schlegel, A., Scherer, P. E., and Lisanti, M. P. (1998) *J. Biol. Chem.* **273,** 5419–5422.
10. Engelman, J. A., Wykoff, C. C., Yasuhara, S., Song, K. S., Okamoto, T., and Lisanti, M. P. (1997) *J. Biol. Chem.* **272,** 16374–16381.
11. Li, S., Couet, J., and Lisanti, M. P. (1996) *J. Biol. Chem.* **271,** 29182–29190.
12. Couet, J., Li, S., Okamoto, T., Ikezu, T., and Lisanti, M. P. (1997) *J. Biol. Chem.* **272,** 6525–6533.
13. Glenney, J. R., Jr. (1989) *J. Biol. Chem.* **264,** 20163–20166.
14. Koleske, A. J., Baltimore, D., and Lisanti, M. P. (1995) *Proc. Natl. Acad. Sci. USA* **92,** 1381–1385.
15. Galbiati, F., Volonte, D., Engelman, J. A., Watanabe, G., Burk, R., Pestell, R. G., and Lisanti, M. P. (1998) *EMBO J.* **17,** 6633–6648.
16. Liu, P., Ying, Y., and Anderson, R. G. W. (1997) *Proc. Natl. Acad. Sci. USA* **94,** 13666–13670.
17. Engelman, J. A., Chu, C., Lin, A., Jo, H., Ikezu, T., Okamoto, T., Kohtz, D. S., and Lisanti, M. P. (1998) *FEBS Lett.* **428,** 205–211.
18. Lee, S. W., Reimer, C. L., Oh, P., Campbell, D. B., and Schnitzer, J. E. (1998) *Oncogene* **16,** 1391–1397.
19. Volonte, D., Galbiati, F., and Lisanti, M. P. (1999) *FEBS Lett.* **445,** 431–439.
20. Yuspa, S. H., Hawley-Nelson, P., Koehler, B., and Stanley, J. R. (1980) *Cancer Res.* **40,** 4694–4703.

21. Maeda, N., Niinobe, M., Nakahira, K., and Mikoshiba, K. (1988) *J. Neurochem.* **51,** 1724–1730.
22. Tobey, R. A., Valdez, J. G., and Crissman, H. A. (1988) *Exp. Cell Res.* **179,** 400–416.
23. Fujimoto, T., Nakade, S., Miyawaki, A., Mikoshiba, K., and Ogawa, K. (1992) *J. Cell Biol.* **119,** 1507–1513.
24. Dupree, P., Parton, R. G., Raposo, G., Kurzchalia, T. V., and Simons, K. (1993) *EMBO J.* **12,** 1597–1605.
25. Fishkind, D. J., and Wang, Y. L. (1995) *Curr. Opin. Cell Biol.* **7,** 23–31.
26. Narumiya, S. (1996) *J. Biochem. Tokyo* **120,** 215–228.
27. Kishi, K., Sasaki, T., Kuroda, S., Itoh, T., and Takai, Y. (1993) *J. Cell Biol.* **120,** 1187–1195.
28. Yasui, Y., Amano, M., Nagata, K., Inagaki, N., Nakamura, H., Saya, H., Kaibuchi, K., and Inagaki, M. (1998) *J. Cell Biol.* **143,** 1249–1258.
29. Madaule, P., Eda, M., Watanabe, N., Fujisawa, K., Matsuoka, T., Bito, H., Ishizaki, T., and Narumiya, S. (1998) *Nature* **394,** 491–494.
30. Michaely, P. A., Mineo, C., Ying, Y., and Anderson, R. G. W. (1999) *J. Biol. Chem.* **274,** 21430–21436.
31. Lisanti, M. P., Scherer, P. E., Vidugiriene, J., Tang, Z., Hermanowski Vosatka, A., Tu, Y. H., Cook, R. F., and Sargiacomo, M. (1994b) *J. Cell Biol.* **126,** 111–126.
32. Nomura, R., and Fujimoto, T. (1999) *Mol. Biol. Cell* **10,** 975–986.
33. Parton, R. G., Joggerst, B., and Simons, K. (1994) *J. Cell Biol.* **127,** 1199–1215.
34. Lucocq, J., Warren, G., and Pryde, J. (1991) *J. Cell Sci.* **100,** 753–759.
35. Scheiffele, P., Verkade, P., Fra, A. M., Virta, H., Simons, K., and Ikonen, E. (1998) *J. Cell Biol.* **140,** 795–806.